

Local Pulsars; A note on the Birth-Velocity Distribution¹

A. Blaauw² & R. Ramachandran³

² Department of Astronomy, Kapteyn Institute, P.O.Box 800, 9700 AV Groningen, The Netherlands.

³ Astronomical Institute "Anton Pannekoek", Kruislaan 403, 1098 SJ Amsterdam, The Netherlands.

Abstract. We explore a simple model for the representation of the observed distributions of the motions, and the characteristic ages of the local population of pulsars. The principal difference from earlier models is the introduction of a unique value, S , for the kick velocity with which pulsars are born. We consider separately the proper motion components in galactic longitude and latitude, and find that the distributions of the velocity components parallel and perpendicular to the galactic plane are represented satisfactorily by $S = 200$ km/sec, and leave no room for a significant fraction of much higher velocities. The successful proposition of a unique value for the kick velocity may provide an interesting tool in attempts to understand the physical process leading to the expulsion of the neutron star.

1 Introduction; the Model used

The early proper motion measurements have indicated that pulsars, on the average, have spatial velocities of the order of a few hundred km/sec (Lyne, Anderson & Salter 1982). Subsequent measurements, over the past 15 years have provided evidence for speeds as high as a thousand km/sec (Bailes *et al.* 1990; Fomalont *et al.* 1992; Harrison *et al.* 1993). Many models have been suggested to explain the spatial velocities of pulsars. Harrison & Tadimaru (1975) proposed the "rocket" theory which essentially stated that the pulsar is accelerated along the magnetic axis due to the radiation reaction soon after it was born. However, subsequent observations have failed to confirm the prediction of the model, that there is an alignment between the directions of proper motion and the magnetic axis. Gott, Gunn & Ostriker (1970) proposed that pulsars derive their spatial velocities from their progenitor binary systems, when the binary disrupts due to the heavy mass loss during the supernova explosion (Blaauw 1961). Asymmetric supernova explosions were proposed by Shklovskii (1970). No fully satisfactory theory has been proposed yet.

Clearly, knowledge of the shape of the birth-velocity distribution is of basic importance for any theory that attempts to clarify the mechanism that causes the birth-velocities. The present paper is concerned with this problem. Among the most recent hypotheses for the birth-speed distribution are those by Lyne & Lorimer (1993) and Hansen & Phinney (1997), shown in figure 1. Hartman (1997) finds that a velocity distribution that has many more pulsars at low velocities than that of Lyne & Lorimer also describes the observations quite well.

Whereas these distributions are characterised by maximum density in velocity-space near zero-velocity, we assume all pulsars to have been ejected from the parent body with the same birth speed – henceforth denoted by S – isotropically distributed. Accordingly, in velocity space, velocity vector points define a spherical surface with radius S . We consider such an alternative worth exploring because it cannot be excluded at this stage of pulsar physics, that the birth (kick) velocities are spread around a (physically) preferred value rather different from zero. With regard to the space distribution of the progenitors, we assume these to be located in a layer of zero thickness at $z = 0$. This assumption is rather harmless because it is generally agreed that pulsars originate from the massive stars in the Galaxy which are confined to a layer the thickness of which is very small as compared to the scale-height of the z -distribution of the pulsars. Finally we assume an upper limit to the age, T , and we do not consider for this analysis pulsars with ages greater than T . Accordingly,

¹This paper is an extended analysis of the talk presented by AB at the Raman Research Institute on 20th February, 1996.

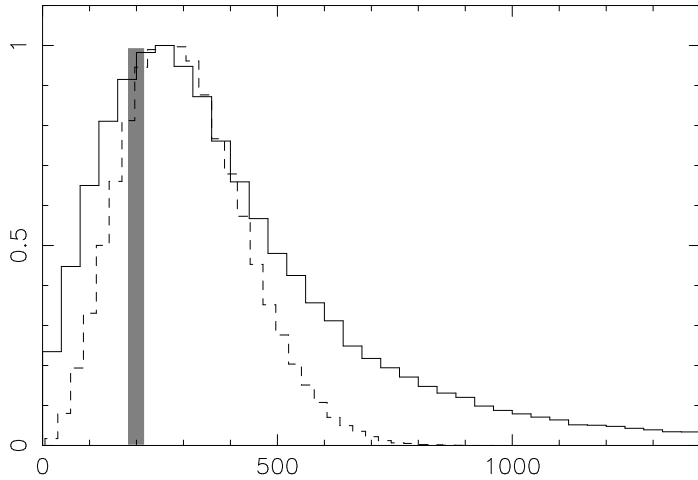


Figure 1: The birth speed distribution of pulsars as predicted by Lyne & Lorimer (1993) (solid line) and Hansen & Phinney (1997) (dash line), and as explored in the present paper (gray bar).

the quantity to be solved for will be only S . Our analysis also differs from previous ones in that we separately consider the velocity components parallel and perpendicular to the galactic plane.

Naturally, the assumed uniqueness of the birth speed cannot but be an approximation of the true situation, for even if there is uniqueness in the kick velocities with which the pulsars leave the parent body, these are vectorially added to the space motion of the parent body, i.e., in the case of components of binary systems, the orbital velocity and the systemic velocity. This implies that the birth-speed distribution is not a delta function but exhibits a certain width. However, since the birth speed we arrive at, $S = 200$ km/sec, generally dominates over these vector additions, the simplified model remains a good first approximation.

In section 2 we give analytical expressions for the expected distributions, and demonstrate why the pulsar velocities parallel to the plane provides a direct way to estimate the velocity S . The observed pulsar population suffers from severe selection effects, which must be taken into account when comparing theoretical and observed distributions. We have done this through a detailed Monte Carlo simulations described in section 3.

We compare our model with observations for the cylindrical volume of space defined by $|z| < 1$ kpc and projected distances $d \cos b$ smaller than 2 kpc only. Within this volume we assume steady state for velocity and space distribution.

2 Definitions and analytical relations

We denote by,

S , the (unique) three dimensional speed at birth of the neutron star. In our analysis this will be the velocity with respect to the local standard of rest at the position of the Sun.

T , the (adopted) upper limit to the pulsar age; only those pulsars with characteristic ages less than T are considered for this analysis.

z , the distance from the galactic plane,

$K(z)$, the acceleration perpendicular to the plane due to the galactic gravitational field; K will be counted positive in the direction towards the plane,

d , the distance from the Sun,

w , the velocity component perpendicular to the galactic plane,

w_0 (km/sec)	10	20	30	40	50	60	70	80	90	100
z_{\max} (kpc)	0.12	0.27	0.45	0.68	0.95	1.22	1.56	1.90	2.21	2.6
$T_{1/4}$ (Myr)	18	21	25	28	31.5	35	38	40	42	43.5

Table 1: The maximum height from the galactic plane (z_{\max}) and the quarter oscillation time ($T_{1/4}$) for various initial z -velocities (w_0).

w_0 , the value of w at birth,

v , the velocity component (parallel to the plane) corresponding to the proper motion component in galactic longitude,

$G(S)$, the number of neutron stars generated per unit time per unit surface at $z = 0$,

$G_0(w_0) dw_0$, the number among these in the interval $w_0, w_0 + dw_0$. Since the velocities at birth are distributed isotropically, this is a flat distribution:

$$G_0(w_0) dw_0 = G(S) dw_0 / S = C dw_0, \quad (1)$$

$G_z(w)$ dw , the number passing level z with velocities $w, w + dw$ per unit surface per unit time. We assume symmetry with respect to the galactic plane, hence the model deals only with positive values of z and w .

There is a subset of the pulsar population moving toward the plane after having reached maximum distance z . Table 1 gives this maximum distance, z_{\max} for various values of w_0 , and the quarter oscillation times $T_{1/4}$, computed with the adopted force field described in section 3.1. Objects with w_0 below about 52 km/sec remain during their full lifetime below $z = 1$ kpc and hence, within the volume of space we study. For $S = 200$ km/sec these represent about one quarter of the population. For $T = 50$ Myr, roughly one half of them will be observed also after they have reached maximum distance from the plane. Objects with w_0 in excess of 50 km/sec will orbit beyond $z = 1$ kpc and re-enter the lower domain on their way back. In these upper parts of their orbits they dwell relatively long: for $w_0 = 60$ km/sec they re-enter only at the age of about 50 Myr, for larger w_0 they dwell even longer beyond 1 kpc. Hence, it is only in the interval of w_0 between 52 and 60 km/sec that we expect to find objects younger than 50 Myr to re-appear in the domain below $z = 1$ kpc. Summarizing, for $T = 50$ Myr, a small fraction of the observed population, about 15 percent, will be on their way back to the plane. For lower values of T , this percentage is accordingly lower. The simulations take their presence into account.

2.1 Velocities perpendicular to the plane

The space density of neutron stars at $z = 0$ with $w_0, w_0 + dw_0$ is

$$D_0(w_0) dw_0 = (1/w_0) G_0(w_0) dw_0 = (C/w_0) dw_0. \quad (2)$$

Since

$$w^2 = w_0^2 - 2 \int_0^z K(z) dz \quad (3)$$

for objects to reach level z , a minimum value of w_0 , denoted by w_{\min} is required:

$$\begin{aligned} w_{\min}^2 &= 2 \int_0^z K(z) dz = 2P(z) \\ \text{Where, } P(z) &= \int_0^z K(z) dz. \end{aligned} \quad (4)$$

The range of values w_0^2 for objects reaching level z and beyond is:

$$\text{Range in } w_0^2 = S^2 - w_{\min}^2 \quad (5)$$

This is also the range of the corresponding values w^2 at level z , since w_{\min} becomes zero and S becomes w_s ,

$$\text{where } w_s^2 = S^2 - 2 \int_0^z K(z) dz = S^2 - 2P_z = S^2 - w_{\min}^2 \quad (6)$$

However, the range of w at level z , *i.e.*, from zero to w_s , is broader than the corresponding range at birth in the ratio $w_s/(S - w_m)$. For instance, if we assume $S=180$ km/sec, for reaching level 420 pc, w_0 should range from 30 to 180 km/sec, *i.e.*, 150 km/sec, whereas the resulting range at level $z=420$ pc becomes $w = 0$ to $w_s = 177$ km/sec.

Since for given z , from equation 3, $\Delta w^2 = \Delta_0(w_0^2)$, we have, $w_0 \Delta w_0 = w \Delta w$. Hence, the broadening for given w is in the ratio w_0/w .

Accordingly, whereas $G_0(w_0) dw$ is flat, for a given level z , $G_z(w) dw$ is proportional to w/w_0 , with w and w_0 related by equation 3.

The number of objects per unit volume at level z with w in the interval $w, w + dw$ will be,

$$D_z(w) dw = (1/w)G_z(w) dw. \quad (7)$$

Due to the broadening just mentioned,

$$G_z(w) = (w/w_0)G_0(w_0) \quad (8)$$

Hence, $D_z(w) = (C/w_0)$, and we have the well known relation, $D_z(w) = D_0(w_0)$ for pairs of values w and w_0 related by equation 3.

The above relations do not take into account the disappearance from the sample of the pulsars older than age T . We denote by w_t the minimum velocity at $z = 0$ required for reaching level z within the time-span T . w_t is defined by:

$$T = \int_0^z \frac{dz}{w(z)} = \int_0^z \frac{dz}{\sqrt{w_t^2 - 2P}}. \quad (9)$$

Thus, there is an interval of velocities at level z from zero to w_z , in which no objects will occur. Again, we have,

$$w_z^2 = w_t^2 - 2P$$

Accordingly, at level z , the distribution of velocities w can be described by the above $D_z(w) dw$ truncated at the low velocity end by eliminating the interval $w = 0$ to $w = w_z$.

Figures 2 demonstrate this effect. They have been obtained numerically for an adopted value $S = 180$ km/sec and $T = 8$ Myr. The five histograms correspond to five different z -slabs (between 0 and 1 kpc), each of width 200 pc. In the highest layer we note the absence of pulsars in the velocity range $w = 0$ to 90 km/sec. At lower z -levels the empty interval is accordingly smaller. At the high-velocity end the limiting velocity w_l is fixed by $w_l^2 = (S^2 - 2P)$. The fact that the cut-off is not sharp is due to the combination of all z -values within the slab.

2.2 Velocities parallel to the plane

We denote by,

v , the component of the velocity parallel to the galactic plane corresponding to the proper motion in galactic longitude:

$$v = d \mu_l \cos b$$

Since the distribution of v is symmetric we consider only the absolute value of v . At level z , for a given T , v ranges from 0 to $v_l = (S^2 - w_t^2)^{1/2}$. The predicted distribution will be shown to be:

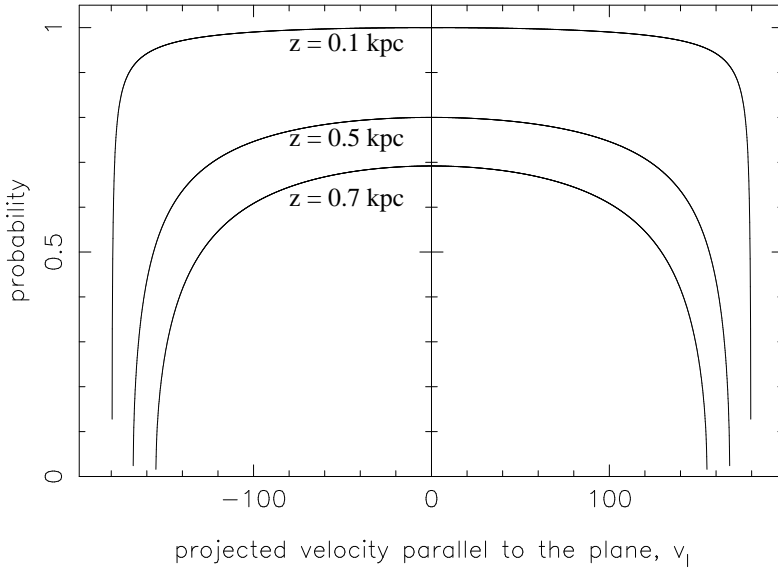


Figure 3: Distribution of velocities $D(v)$ parallel to the plane, as given by equation 10. The three curves correspond to $z = 0.1, 0.5 \& 0.7$ kpc, respectively, for $S = 180$ km/sec and $T = 8$ Myr.

$$D(v) \, dv = C' S \left\{ \pi/2 - \arcsin \left[\frac{w_t}{\sqrt{S^2 - v^2}} \right] \right\} \, dv \quad (10)$$

where C' is a constant defined below.

We define by $N(v, w)$ the number of objects at level z per unit of v and of w . Equation 10 then follows from

$$D(v) \, dv = dv \int_{w_t}^{w_l} N(v, w) \, dw = dv \int_{w_t}^{w_l} N(0, w) \frac{R \, dw}{\sqrt{R^2 - v^2}}$$

where, $R^2 = (S^2 - w^2)$, $w_l^2 = (S^2 - v^2)$, and $N(0, w) = N(0, 0) S / \sqrt{S^2 - v^2}$, so that,

$$\begin{aligned} D(v) \, dv &= dv S N(0, 0) \int_{w_t}^{w_l} \frac{dw}{\sqrt{S^2 - v^2 - w^2}} \\ &= S N(0, 0) \left[\pi/2 - \arcsin \frac{w_t}{\sqrt{S^2 - v^2}} \right] \, dv. \end{aligned}$$

where $C' = N(0, 0)$ is the number per unit v and unit w at $v = 0$, $w = 0$ at $z = 0$.

For low z -levels the distribution $D(v) \, dv$ is nearly flat up to v close to v_l . This is due to the fact that the second term in equation 10 becomes significant with respect to the first, constant term, only at high v . For instance, for $S = 200$ km/sec and $T = 20$ Myr, at $v = 0.9v_l$, the ratio between the second and the first term near $z = 0$ is only 0.036. For high z -levels the distribution becomes less flat. Figure 3 demonstrates this effect. As we chose higher values of T , the nature of the curves for higher z becomes more similar to the one for the lowest z . The truncated nature of $D(v)$, particularly at low z , provides an important tool in estimating S ; the extreme observed value, v_l is an approximate measure of S virtually independent of the assumed life time T .

3 Simulations

We did a Monte Carlo simulation to generate a large number of objects in the solar neighbourhood (with initial value of $z=0$), keeping the surface density constant. As mentioned in the previous sections, we assumed a simplistic model with all neutron stars being ejected out isotropically with a constant speed (S). This assumption corresponds to having initial velocities in the z -direction ranging from zero to S with uniform probability. We evolve them in an assumed local gravitational potential to get their velocity and spatial distributions, and in addition we studied the distributions of their characteristic ages. Each object was assigned an age chosen randomly with uniform probability between zero and T . Given the distribution of characteristic ages of known pulsars, we chose a value of $T = 50$ Myr as an optimal choice in order to include a sufficiently large sample, and at the same time describe the kinematics with our potential model. The presence of the objects which turn over after reaching their maximum z -amplitude of oscillation within their age are accounted for.

3.1 Local gravitational potential

To study the kinematics of the generated objects we assumed the local gravitational potential function given by Kuijken & Gilmore (1989). The vertical acceleration due to this potential is given by (Bhattacharya *et al.*)

$$g_z = 1.04 \times 10^{-3} \left[\frac{1.26 z}{\sqrt{z^2 + 0.18^2}} + 0.58 z \right] \quad (11)$$

where g_z is in units of kpc/Myr² and z in kpc. We use this function to evolve every one of the generated objects from their initial position and velocity to their current value after a time t .

3.2 Further assumptions for simulation

We assumed a Gaussian distribution of fields in logarithmic scale, with $\langle \log B(G) \rangle = 12.2$ with a root mean square spread around the mean of 0.3. The choice of initial periods will be discussed in section 4.4. With an assumption that the magnetic field does not decay significantly within the time scales of our interest (~ 50 Myr) the final rotational period of the pulsar can be easily calculated with the simple dipole formula

$$B^2 = \frac{3Ic^3}{8\pi R^6} P \dot{P} \quad (12)$$

where c is the velocity of light, I is the moment of inertia of the neutron star, and \dot{P} is the time derivative of the rotation period P .

The simulation was repeated for various values of S (ranging from 90 km/sec to 350 km/sec) and T (from 15 Myr to 50 Myr). At the end of the evolution, pulsars which have the quantity $(B/P^2) < 2 \times 10^{11}$ were neglected from the simulation, since it is believed that the pulsar activity ceases to continue below this limit.

3.3 Selection filter

After evolving the generated objects in the galactic potential, their final position, velocity components, rotation period and characteristic age are noted down. After compensating for observational selection effects a subset of this population was selected to compare with the known sample. The procedure we have adopted for this task is the same as the one described by Deshpande *et al.* (1995). We selected only those pulsars which are, in principle, detected by any one of the eight major pulsar surveys considered, namely (1) Jodrell Bank survey, (2) U. Mass–Arecibo survey, (3) Second Molonglo survey, (4) U. Mass–NRAO survey, (5) Princeton–NRAO Phase I survey, (6) Princeton–NRAO Phase II survey, (7) Princeton–Arecibo survey, and (8) Jodrell Bank–1400 MHz survey. Since our analysis

deals with only the solar neighbourhood (projected distance onto the plane less than 2 kpc, and $|z| < 1$ kpc) the effect due to interstellar scattering and dispersion are ignored. While comparing the results of the simulation with the known sample, only the subset of the simulated sample (*detectable* simulated sample) was used.

For consistency, even the sample of known pulsars were passed through this filter to select a subsample, which was finally used for comparison with the simulated sample.

4 Comparison with observations

4.1 Velocities parallel to the plane

As the first step, we consider the distribution of velocity components parallel to the plane, $D(v)$, because as it was explained in section 2.2, these provide the estimate of S . From the compilation of Taylor *et al.* (1995) we use those proper motion measurements for which the quantity $d \times \sigma < 94$ km/sec (20 A.U./yr), where σ is the formal error in the proper motion quoted by those authors. We do not apply corrections for solar motion and differential galactic rotation, since within the range of distances considered, these are negligible as compared to the true proper motions and their observational errors. Figure 4(a) gives the distribution of these velocities, and figure 4(b) gives their distribution as a function of the height from the galactic plane. We note that with the exception of 5 objects, all are confined within ± 210 km/sec. In comparison with figure 3 we may conclude that the value of the unique velocity must be roughly around about 200 km/sec. Clearly, values of S in excess of 250 km/sec are incompatible with the proper motions.

4.2 Density Distribution perpendicular to the plane

Hartman & Verbunt (1994), from their study of evolution of neutron stars in various models of the local gravitational potential, demonstrate the effect of observational selection for understanding the distribution of pulsars perpendicular to the plane. Since observations tend to detect more luminous pulsars (which are younger and closer to the plane), irrespective of the nature of the *true* distribution the *observable* distribution is roughly the same. This has been seen in our simulations too. While comparing the simulated sample (after compensating for the selection effects) with the observed, a satisfactory Kolmogorov – Smirnov probability was achieved for many different combinations of S and T . For $S = 180$ km/sec and $T = 50$ Myr (figure 5) the K–S probability was 59.6%, and for many other combinations of (S, T) , like (250,50), (350,50) the K–S probability was roughly as high as for (180,50). Therefore, one can conclude that the density distribution perpendicular to the galactic plane alone is not a severe constraint on the kinematic properties of pulsars, and one needs to study other properties like the velocity components and the distribution of characteristic ages, etc.

4.3 Velocities perpendicular to the plane

We do not have measured w , since there is no way of measuring the radial component of the velocity vector. However, for pulsars with sufficiently low galactic latitude (say, $|b| < 50^\circ$), we can approximate $w = \mu_b \times d$ provided $\cos b$ is close to unity. Out of the 30 pulsars selected, 23 have $\cos b > 0.87$, 5 have $\cos b = 0.78 – 0.87$, and 2 have $\cos b = 0.72 – 0.78$. Figure 6(a) gives the distribution of $(\mu_b \times d)$. Figure 6(b) shows the distribution of $\mu_b \times d$ against the height from the galactic plane. Objects at negative z are plotted with reversed z and reversed $\mu_b \times d$. The asymmetry in the distribution of $\mu_b \times d$ in figure 6(a) shows the flow of objects away from the galactic plane.

Once a considerably richer sample of accurate pulsar proper motions is available, it will be of great interest to make the detailed comparison between the observed distribution and the theoretical one of figure 2, and check its rapidly varying shape with increasing z . The predicted run of the mean velocity v with increasing z is in harmony with observations, as shown in figure 6(b).

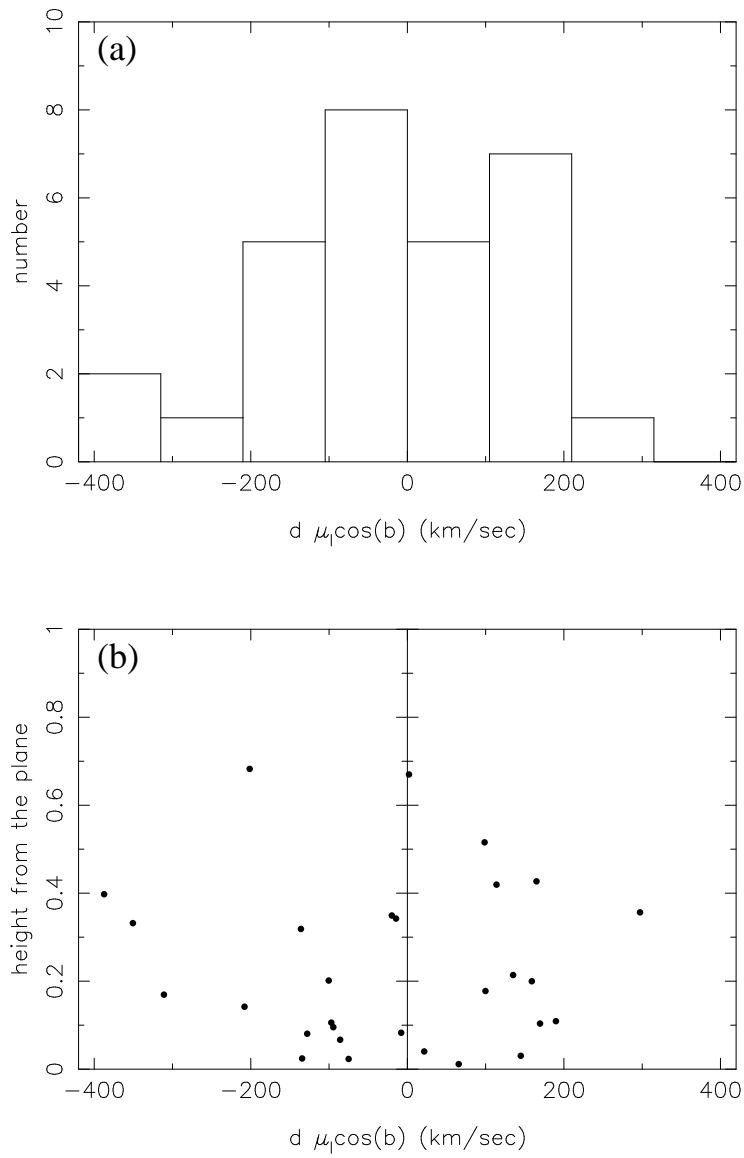


Figure 4: Velocities parallel to the plane corresponding to the proper motions in galactic longitude. (a) Distribution of these velocities, (b) Distribution of velocities as a function of height from the galactic plane. Only those pulsars whose proper motion errors (1σ) are less than 94 km/sec (20 A.U./yr) are considered for this figure.

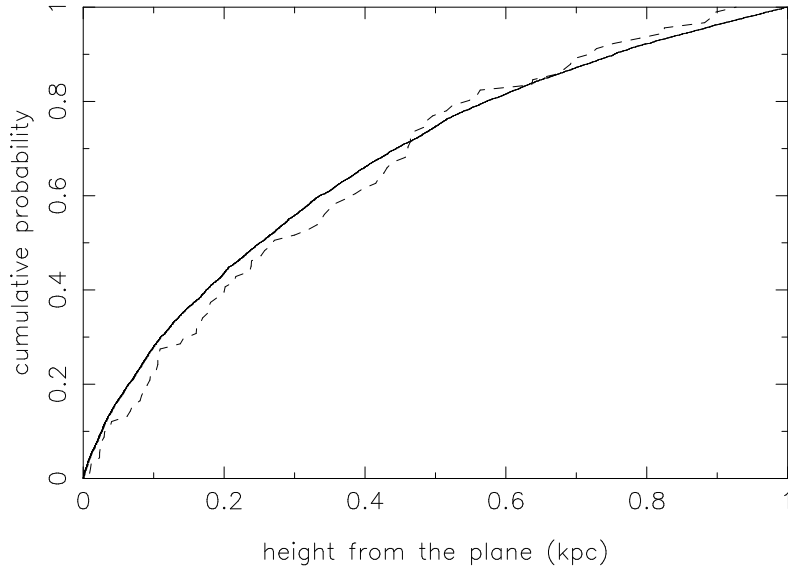


Figure 5: The cumulative number distribution of pulsars as a function of height from the galactic plane. Dash line is for the known sample and the solid line is the best fit corresponding to $S = 180$ km/sec and $T = 50$ Myr.

4.4 Distribution of characteristic ages

As described in section 3.2 we have assumed that the magnetic fields at birth are distributed as a Gaussian in $\log B$ around 12.2 with an r.m.s. of 0.3. Since many of the earlier works (Vivekanand & Narayan 1981; Srinivasan *et al.* 1984; Narayan 1987; Narayan & Ostriker 1990; Deshpande *et al.* 1995) suggest that pulsars are born with rotation periods as long as a few hundred milliseconds, for the simulation, all pulsars were assumed to be born with rotation period of 0.1 sec. With the assumption that the magnetic field does not decay with time, the period was evolved with the simple dipole formula 12. Objects were evolved in the local gravitational potential for their corresponding ages (distributed between zero and T with uniform probability). At the end of the simulation pulsars with $B/P^2 < 2 \times 10^{11}$ Gs $^{-2}$ were neglected, since the pulsar activity is believed to cease below this limit. After applying the *selection effect filter*, a subset of the simulated sample (detectable subset of the simulated sample) was selected for comparison with the known sample.

Figure 7 gives the distribution of known pulsars in the $z - \log \tau_{\text{ch}}$ plane (where τ_{ch} is the characteristic age of the pulsar). The ‘dash’ line gives the observed mean value of $\log \tau_{\text{ch}}$ in the five different z -slabs from zero to 1 kpc, and the solid line gives the corresponding mean value of the “detectable” simulated sample for the combination of $S = 180$ km/sec and $T = 50$ Myr. The “dotted” line gives the possible lower limit of τ_{ch} for a given height from the plane. *i.e.*, with initial velocities, w_0 , ranging from zero to S , the object can reach a given height z , only if its age is greater than a certain value.

As one can see from this figure, our model fits with the observed distribution of $\log \tau_{\text{ch}}$ as a function of z , quite satisfactorily. The fact that the envelope in figure 7 (given by the dotted line) encloses all the pulsars means that almost all pulsars are born close to the plane and they migrate by the virtue of their velocities. As it turns out, to constrain the combination of S and T , the distribution of $\log \tau_{\text{ch}}$ can be used effectively.

Ideally we would have liked to compare the distribution of $\log \tau_{\text{ch}}$ in each z -slab with the corresponding observed distribution. However, small number of the observed sample prevents us from doing so.

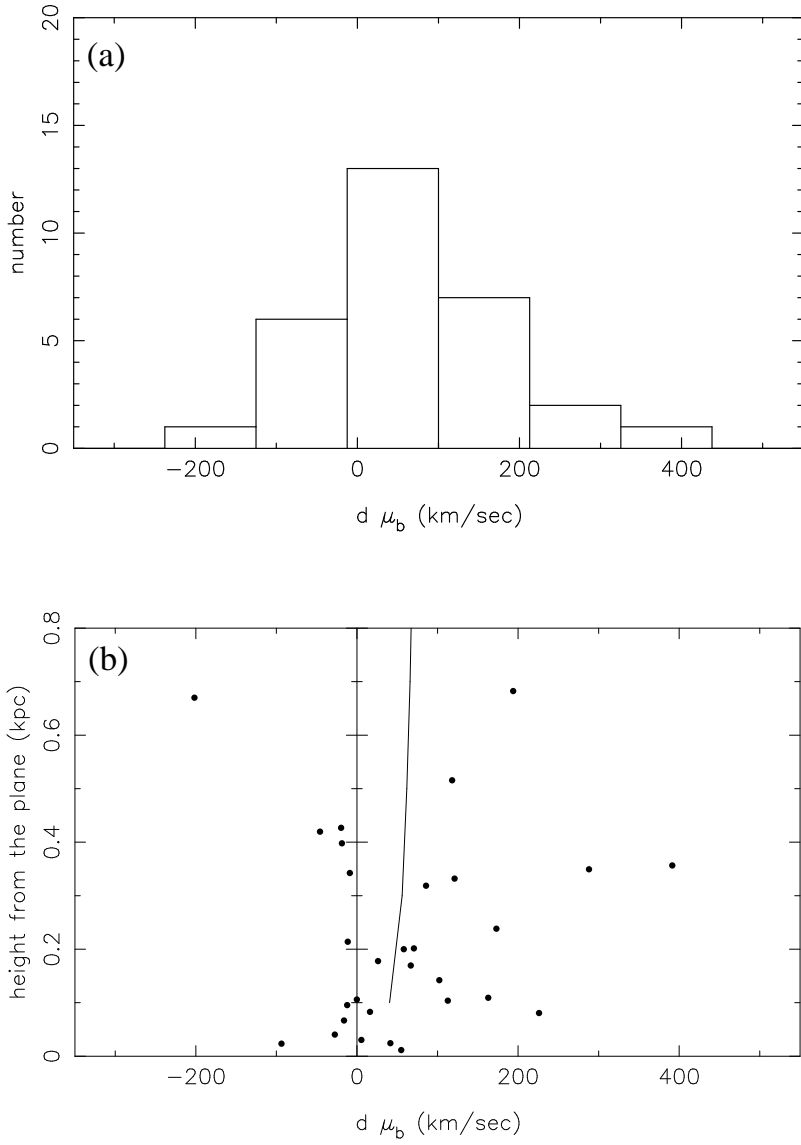


Figure 6: (a) Distribution of $d \times \mu_b$ of known pulsars, (b) distribution of known pulsars as a function of $d \times \mu_b$ and the height from the plane. Only those pulsars with $|b| < 50^\circ$ and velocity error less than 94 km/sec are included. The solid line gives the mean of the simulated sample for $S = 180$ km/sec., $T = 50$ Myr.

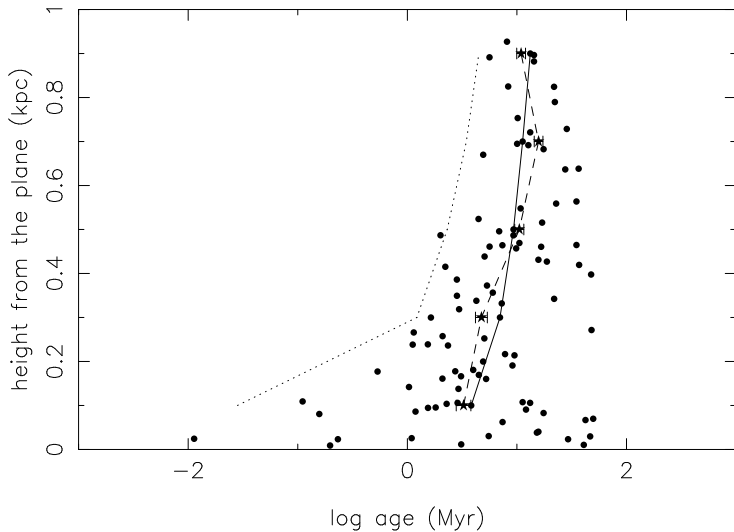


Figure 7: Distribution of known pulsars in $z - \log \tau_{\text{ch}}$ plane. The dash line indicates the average $\log \tau_{\text{ch}}$ as a function of z , for the known sample. Solid line indicates the corresponding quantity for the simulated sample for $S=180$ km/sec and $T=50$ Myr. The dotted lines give the predicted lower bound for τ_{ch} as a function of z . The error bars indicate the uncertainty in the mean value.

5 Conclusions

We have explored the hypothesis that pulsars are born in the galactic plane with a unique kick velocity S , distributed isotropically. We therefore investigate the pulsars in the solar neighbourhood by studying the distributions of the velocity components parallel and perpendicular to the galactic plane, and the characteristic age distribution. We find that the known sample of pulsars in the solar neighbourhood is consistent with kick velocities of about 200 km/sec.

We wish to emphasize that our analysis of the nearby pulsars leaves no room for the existence of an appreciable fraction of pulsars with velocities much higher than 200 km/sec. These should have shown up in the plots of figures 4 & 6. Evidence for very high velocities came from a few reliable proper motion measurements (Bailes *et al.* 1990; Harrison *et al.* 1993; Fomalont *et al.* 1992) and velocities inferred from the association of a few pulsars with supernova remnants (Caraveo 1993; Frail, Goss & Whiteoak 1994). The reliability of such associations has been questioned by Kaspi(1996).

The analysis by Brandt & Podsiadlowski (1995) shows that the assumed kick speeds of the order of 450 km/sec are inconsistent with the eccentricity – orbital period distribution of binaries which contain neutron stars, and it is consistent with kick speeds of 200 km/sec. This supports our result.

The velocity distribution derived by Lyne & Lorimer (1993) and Hansen & Phinney (1997), referred to in the introduction and figure 1, show a considerable fraction of pulsars with velocities around 200 km/sec, the value of S we arrived at. They differ from our model in two respects:

1. Both of them show maximum density in velocity space around velocity zero, whereas our model gives zero density at zero velocity.
2. Both of them show a long tail towards the high-speed end. This is recognised in our plots of the velocity components v and w (figures 4 & 6), but this represents a small fraction only of the total distribution.

The recent paper by Fomalont *et al.* (1997) has brought out improved proper motion measurements for about 15 pulsars. Among those pulsars with distance less than 2 kpc and galactic latitude less than 50 degrees, on the basis of the earlier measurements we had ignored 1556–44 & 1749–28, since they had

errors greater than 20 A.U./yr. For 1919+21 & 2045–16 the improved proper motion measurements seem to be quite different from the earlier measurements. However, since these changes are unlikely to change the results in this paper we have done our analysis on the basis of the earlier measurements.

To summarise the main result, we show that if pulsars are postulated to derive a unique isotropic supernova kick speed at their birth around 200 km/sec, the distribution of the proper motions and the characteristic ages of pulsars in the solar neighbourhood can then be understood satisfactorily.

Acknowledgement

We would like to thank Dipankar Bhattacharya for his very valuable comments which have helped us a great deal to improve the manuscript.

References

1. Bailes M., Manchester R.N., Kastevan M.J., Norris R.P. & Reynolds J.E. 1990, Monthly Notices Roy. Astr. Soc., 247, 322
2. Bhattacharya D., Wijers R.A.M.J., Hartman J.W. & Verbunt F. 1991, Astron. Astrophysics, 254, 198
3. Blaauw A. 1961, Bull. Astr. Inst. Netherlands, 15, 265
4. Brandt N. & Podsiadlowski P. 1995, Monthly Notices Roy. Astr. Soc., 274, 461
5. Caraveo P.A. 1993, Astrophys. J., 415, L111
6. Deshpande A.A., Ramachandran R. & Srinivasan G. 1995, J. Astrophys. Astr., 16, 53
7. Fomalont E.B., Goss W.M., Lyne A.G., Manchester R.N. & Justtanont K. 1992, Monthly Notices Roy. Astr. Soc., 258, 497
8. Fomalont E.B., Goss W.M., Manchester R.N. & Lyne A.G. 1997, Monthly Notices Roy. Astr. Soc., 286, 81
9. Frail D.A., Goss W.M. & Whiteoak J.B.Z. 1994, Astrophys. J., 437, 781
10. Gott J.R., Gunn J.E. & Ostriker J.P. 1970, Astrophys. J., 160, L91
11. Hansen B.M.S. & Phinney E.S. 1997, Monthly Notices Roy. Astr. Soc., 291, 569
12. Harrison P.A., Lyne A.G. & Anderson B. 1993, Monthly Notices Roy. Astr. Soc., 261, 113
13. Harrison E.R. & Tademaru E. 1975, Astrophys. J., 201, 447
14. Hartman J.W. 1997, Ph.D. thesis, Utrecht University
15. Kaspi V.M. 1996, in Johnston S., Walker M.A., Bailes M. eds., ASP Conf. Ser. Vol. 105, Pulsars: Problems & Progress. Astron. Soc. Pac. San Francisco, P.375
16. Kuijken K. & Gilmore G. 1987, Monthly Notices Roy. Astr. Soc., 239, 571
17. Lyne A.G. & Lorimer D.R. 1993, Nature, 369, 127
18. Lyne A.G., Anderson B. & Salter M.J. 1982, Monthly Notices Roy. Astr. Soc., 201, 503
19. Narayan R. 1987, Astrophys. J., 319, 162.
20. Narayan R. & Ostriker J.P. 1990, Astrophys. J., 352, 222.

21. Shklovskii I.S. 1970, *Astr. Zu.*, 46, 715
22. Srinivasan G., Bhattacharya D. & Dwarakanath K.S. 1984, *J. Astrophys. Astr.*, 5, 403
23. Taylor J.H., Manchester R.N. & Lyne A.G. 1993, *Astrophys. J. Supp.*, 88, 529
24. Vivekakand M. & Narayan R. 1981, *J. Astrophys. Astr.*, 2, 315.

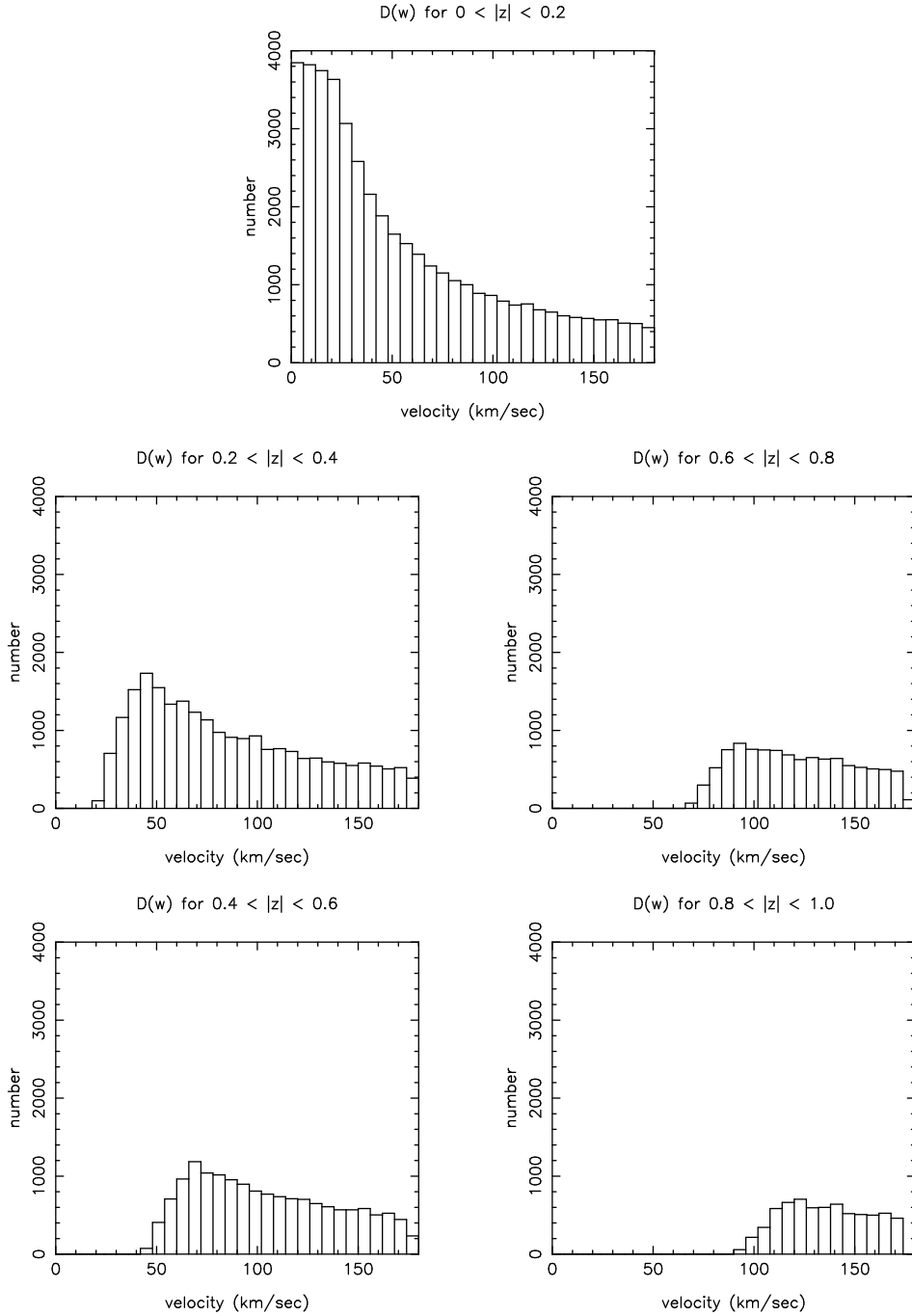


Figure 2: Distribution of velocities perpendicular to the plane of pulsars in different z -slabs after evolving in the potential for ages up to T . This plot corresponds to $S = 180$ km/sec and $T = 8$ Myr.